J Urban Health (2022) 99:134–145
https://doi.org/10.1007/s11524-021-00602-6

Associations Between Historical Redlining and Present-Day Heat Vulnerability Housing and Land Cover Characteristics in Philadelphia, PA

Leah H. Schinasi · Chahita Kanungo · Zachary Christman · Sharrelle Barber · Loni Tabb · Irene Headen

Accepted: 3 December 2021 / Published online: 25 January 2022

Abstract Historical, institutional racism within the housing market may have impacted present-day disparities in heat vulnerability. We quantified associations between historically redlined areas with present-day property and housing characteristics that may enhance heat vulnerability in Philadelphia, PA. We used color-coded Home Owners Loan Corporation (HOLC) maps and tax assessment data to randomly select 100 present-day (2018–2019) residential properties in each HOLC grade area (A = Best; B, C, and D = Most hazardous; $N = 400$ total). We conducted virtual inventories of the properties using aerial and streetview imagery for land cover and housing characteristics (dark roof color, flat roof shape, low or no mature tree canopy, no recently planted street trees) that may enhance heat vulnerability. We used modified Poisson regression models to estimate associations of HOLC grades with the property characteristics, unadjusted and adjusted for historical and contemporary measures of the neighborhood sociodemographic environment. Compared to grade A areas, higher proportions of properties in grade B, C, and D areas had dark roofs, low/no mature tree canopy, and no street trees. Adjusting for historical sociodemographics attenuated associations, with only associations with low or no tree canopy remaining elevated. Adjusting for present-day concentrated racial and socioeconomic deprivation did not substantially impact overall findings. In Philadelphia, PA, HOLC maps serve as spatial representations of present-day housing and land cover heat vulnerability

Supplementary Information The online version contains supplementary material available at https://doi.org/10.1007/s11524-021-00602-6.

L. H. Schinasi (✉) · C. Kanungo
Department of Environmental and Occupational Health, Dornsife School of Public Health, Drexel University, 3215 Market Street, Philadelphia, PA 19104, USA
e-mail: lhs36@drexel.edu

L. H. Schinasi · C. Kanungo · S. Barber · L. Tabb · I. Headen
Dornsife School of Public Health, Urban Health Collaborative, Drexel University, Philadelphia, PA, USA

Z. Christman
Department of Geography, Planning, and Sustainability, School of Earth and Environment, Rowan University, Glassboro, NJ, USA

S. Barber · L. Tabb
Department of Epidemiology and Biostatistics, Dornsife School of Public Health, Drexel University, Philadelphia, PA, USA

I. Headen
Department of Community Health and Prevention, Dornsife School of Public Health, Drexel University, Philadelphia, PA, USA

characteristics. Further analyses incorporating longitudinal data on urban redevelopment, reinvestment, and neighborhood change are needed to more fully represent complex relationships among historical racism, residential segregation, and heat vulnerability.

Introduction

Rising global temperatures coupled with intensive urbanization contributes to dangerously hot urban spaces [1, 2]. This represents a critical public health concern; in the absence of appropriate interventions, by the end of the twenty-first century, extreme heat will cause tens of thousands of excess deaths [3]. Risk of mortality from extreme heat is not distributed equally. Past heat wave events, in Philadelphia, [4] Chicago, [5] and Paris [6] have revealed tremendous inequities in vulnerability, with disproportionate impacts on marginalized racial groups, elderly, and poor populations [7]. Built-environment and land cover are modifiable features that contribute to heterogeneity in exposure intensity or adaptive capacity, and thus, to differences in heat vulnerability [8, 9]. For example, lighter surfaces on roofs, pavement, or buildings may cool neighborhoods because they reflect solar radiation [10]. Likewise, more greenspace, such as grass or trees, may cool through evapotranspiration or by providing shade [1, 11]. Impervious surfaces, such as concrete or asphalt, contribute to micro-urban heat islands [1, 12, 13] because they are often dark in color. This translates to low solar reflectance because they absorb and store heat [14] and lack the evapotransporative properties of vegetation [15]. Housing characteristics, such as roofing color, may also contribute to differences in indoor temperature intensity, and thus to differences in heat vulnerability. It is important to consider the determinants of variable indoor temperatures since most heat-related deaths occur indoors [16, 17], and because most people, and especially the elderly and those with chronic conditions or impaired mobility who may be particularly heat sensitive, spend the majority of their time inside [18]. Past studies have documented racial disparities in the spatial distribution of greenspace, [19] tree canopy, and impervious surfaces [20]. No studies, to our knowledge, have documented disparities in housing characteristics, such as roofing color, that might enhance heat vulnerability. Also, few studies have empirically documented the historical contributors to inequities in built environment features that may confer present-day heat vulnerability.

Redlining is a historical form of institutional racism that contributes to present-day racial residential segregation, [21] a fundamental cause of racial disparities in health and neighborhood environments [22-25]. Redlining refers to maps that the federally sponsored Home Owners' Loan Corporation (HOLC) created in the early 1930s, for cities across the USA [21]. During the new deal era and following the Great Depression, when the USA was in the midst of a foreclosure crisis, the HOLC issued loans to help homeowners avoid losing their homes, or to reacquire their already-lost homes. The HOLC assessed the so-called riskiness of borrowers, and thus their willingness to issue loans, by creating maps that delineated neighborhoods into the following grades: A, or most desirable (color = green); B, slightly less desirable (color = blue); C, declining neighborhoods (color = yellow); D, undesirable (color = red). These grades were assigned, in large part, based on the neighborhood's sociodemographic composition, and areas with high percentages low-income immigrant or Black residents received a grade D rating. Redlining has been linked with present-day adverse health outcomes, including higher rates of emergency department visits for asthma [26], higher risk of adverse birth outcomes [27, 28], and late-stage cancer diagnosis [29]. The pathways underlying links between redlining and present-day population health inequities are hypothesized to include neighborhood disinvestment (e.g., disinvestment in built environment infrastructure) and residential segregation, which, in turn, have critical implications for health-promoting, place-based resources [28]

Here, we explore a built-environment pathway that may explain links between historical redlining and present-day disparities in heat-related morbidity and/or mortality. We empirically estimated associations between HOLC risk grades with present-day built-environment characteristics—housing and land cover features—that might confer heat vulnerability. We used high-resolution aerial orthoimagery and 360° streetside panoramic imagery, accessed via Google Maps and Street View services, to virtually inventory residential properties by human observation. The use of these images allowed us to characterize certain housing features, such as roofing color, or land cover

features, such as recently planted, immature street trees, at the property level. Because these features are not represented in publicly available data sources, our work represents an important contribution to the literature on inequities in heat vulnerability, and links between structural racism and built-environments.

The study setting is Philadelphia, PA, which is one of the most racially segregated cities in the USA [30], a city with a history of tragic heat waves [31], and one in which rates of heat-related mortality are higher in neighborhoods with higher proportion Black residents [8].

Methods

Design

We used an ecologic study design, and the primary unit of observation was present-day residential properties clustered within neighborhoods. In primary analyses, we defined present-day neighborhoods using the 2010 United States census tract boundaries [32]. Census tracts are small, relatively permanent subdivisions of a county or equivalent area, with a population size between 1,200 and 8,000 (optimally 4,000) [32]. As a sensitivity analysis, we redefined neighborhoods using tract boundaries from the 1940s decennial census.

HOLC Maps

We used a publicly available, digitized HOLC "risk" map from the University of Richmond's Mapping Inequality Project [33] to identify HOLC-assigned color-coded risk categories (A–D) across Philadelphia (Supplemental Material 1). The HOLC risk map comprised 253.8 km^2 of land area from the within the boundaries of contemporary Philadelphia; HOLC grade A areas comprised 37.3 km^2, grade B areas comprised 97.5 km^2, grade C areas 50 km^2, and grade D areas comprised 68.6 km^2.

Residential Properties

The City of Philadelphia's Office of Property Assessment inspects properties approximately every 3 years to determine taxes [34]. The assessment data contain latitude and longitude coordinates for every property, an indicator for whether it is residential, and additional attribute information. These data were downloaded from the city of Philadelphia's Open Data portal in year 2016 [34]. We used ArcGIS Pro version 2.8.1 to assign the properties to an HOLC grade area, and to a 2010 census tract. We then created four separate HOLC-grade specific databases containing all properties assigned to the relevant grade. We then used an evenly distributed random real number generator to select 100 residential properties to inventory from each of the four databases (coded A, B, C, or D), resulting in 400 total properties for the analysis. This number of properties represented a minimum of one inventoried residence for every km^2 of the area represented by each HOLC risk category, or 2.7, 1.0, 2.0, and 1.5 properties per km^2 in areas A, B, C, and D, respectively. This number of properties was selected based on consideration of the time it takes to conduct manual virtual inventories, while also aiming to include a sufficient number of properties to be representative of the area and allow statistical contrasts.

Sociodemographic Variables from the 1940s Decennial Census

The HOLC grade assignments were informed, at least in part, by the sociodemographic composition of neighborhoods [21, 35]. As a result, it is possible that present-day housing and land cover characteristics were impacted by neighborhood compositional factors that pre-dated the establishment of the HOLC map. We used data from the 1940 decennial census to adjust for potential confounding by historical sociodemographic neighborhood characteristics. This approach is consistent with other analyses using HOLC grade maps [36, 37]. We assigned the residential properties to the 1940s census tract boundaries using ArcGIS Pro version 2.8.1. We downloaded the 1940 decennial census tract-level counts of residents who were Black and White: total population, counts of adults ages 25 years and older with at least 4 years of high school education, counts of homes without a radio, counts of homes in need of repair, counts of homes without central heat, counts of homes without a refrigerator, counts of homes with more than one person per room, and counts of people ages 14 and older reporting unemployment, from the IPUMS National Historical Geographic Information System [38].

Historical Sociodemographic Measures

We used the 1940s census data to quantify differences in proportions of census tract residents who were White vs. Black as the Index of Concentration at the Extremes (ICE) [28, 39]. Following the methods described by Krieger et al., [39] we calculated the ICE for race as $ICE_i = (W_i - B_i / T_i)$ where W_i is equal to the number of white residents in the census tract i, B_i is the number of Black residents in the census tract i, and T is equal to the total population in the census tract i for whom a race was reported. ICE values range from -1 to 1; a value of -1 indicates that all residents belong to the most deprived group and a value of 1 indicates that all residents belong to the most privileged group.

In addition, we constructed a summary neighborhood score to represent the socioeconomic environment of the 1940s census tract, using seven variables that represented housing conditions and amenities (proportion of homes without a radio, proportion of homes in need of repair, proportion of homes without central heat, proportion of homes without a refrigerator, proportion of homes with more than one person per room); unemployment (proportion of people ages 14 and older reporting being unemployed), and education level (proportion of adults ages 25 and up with fewer than 4 years of high school education). To calculate the summary measure, we calculated a z-score for each variable, and then summed each of the z-score standardized variables. This method of creating a neighborhood socioeconomic score is consistent with methods used in other analyses of neighborhood socioeconomic position [40], and the selection of variables for inclusion was informed by previous HOLC grade analyses that, similarly, adjusted for historical sociodemographics [36, 37].

Contemporary Index of Concentration at the Extremes

Historical redlining may directly impact contemporary racial and socioeconomic segregation, which in turn, may have implications for present-day housing and land cover features. We used 5-year average estimates from the American Community Survey (years 2014–2018) [41, 42] to calculate an ICE measure that combines information on race and household income (contrasting counts of wealthy and white residents with counts of Black and poor residents). This measure has been used previously to measure racialized socioeconomic deprivation [28, 39]. Following methods described by others, [28, 39] we calculated the contemporary ICE measure as $(A_i - D_i)/T_i$, where A_i is defined as the total non-Hispanic white residents of census tract i with a median house income $\geq$ 100,000 USD, D_i is the total non-Hispanic Black residents whose median household income was $<$ 25,000 in the census tract i, and T_i is the total residents in the census tract i for whom race and household income were known [28, 39]. The $100,000 and $25,000 cut-points correspond to the 80th and 20th percentiles of contemporary household income distributions in the USA [28, 39].

Land Cover and Housing Characteristic Inventories

We used aerial and 360° panoramic photographic datasets in Google to conduct virtual inventories of housing and land cover features of the 400 randomly selected residential properties. To conduct the inventories, we manually entered, one by one, the latitude and longitude coordinates of each randomly selected property into a Google Maps search engine. We then recorded the following characteristics of each of the properties, using both aerial and streetside imagery: roof color (dark, light, other); roof shape (flat vs. not flat); presence and amount of mature tree canopy on or immediately adjacent to the property; and presence of immature/newly planted street trees on or immediately adjacent to the property. The selection of housing and land cover features was informed by previous work suggesting that these factors might impact indoor heat exposure intensity or contribute to intra-urban heat islands [9, 43, 44]. Before beginning the inventories, two study personnel developed a structured collection tool. To do so, the researchers examined and discussed various residential areas across the city of Philadelphia and established structured definitions for each measure and categorical response option. After developing the structured form, two study personnel inventoried ten randomly selected properties. After these inventories were conducted, the researchers compared results, discussed discrepancies, and came to an agreement about any discrepancies. One individual then conducted all additional inventories and consulted the second study personnel member about any ambiguities. Google Maps offers

snapshots of the same area, at various points in time. We always used the most recent image available. All images were taken in year 2019, except for one image captured in September 2018. All results from the inventories were entered into the structured Google form. The full form that we used is included in Supplemental Material 2 and is shareable as a Google form upon request of the corresponding author. Within the form, sample photos are shown to illustrate the built-environment characteristics that were inventoried and to show, for example, what is meant by roof shape or immature and mature tree presence.

Data Analysis

The primary explanatory variable was the four-category HOLC grade (A (reference category), B, C, D). The primary outcomes in this analysis were each of the following property characteristics, which we modeled separately in five sets of distinct models: (1) roof color (dark vs, light (ref)); (2) roof shape (flat vs. not flat (ref)); (3) roof shape and color combined (flat and dark vs other (ref)); (4) presence of mature tree canopy on or immediately adjacent to the property (none or < 25% vs more (ref)); and (5) presence of immature street trees or immediately adjacent to the property (none vs. any (ref)).

We estimated associations using modified Poisson generalized estimating equation models with an exchangeable correlation matrix, which accommodated clustering of properties within the 2010 census tracts. We used modified Poisson regression approach with a robust error variance because of convergence issues when we used a log-binomial distribution, and because the outcome was common, making the use of logistic regression models inappropriate [45].

We first ran bivariate models to estimate the crude (unadjusted) associations between the HOLC grade and each of the distinct heat vulnerability characteristics (Models 1A–5A). We then ran models adjusted for the 1940s census tract level socioeconomic environment and racial segregation (ICE) (Models 1B–5B). In a third set of models (Models 1C–5C), we ran models adjusted for present-day measures of racialized economic deprivation, estimated using 2014–2018 American Community Survey ICE measures, which could partly explain (i.e., mediate) associations. As a sensitivity analysis, we reran all models (crude and adjusted), specifying clustering by 1940s rather than the 2010 census tract boundaries. We ran the analyses using the package geepack in R version 4.0.3 [46].

Results

Table 1 provides descriptive statistics on contemporary and historical Philadelphia census tracts, across the entire city, and among those tracts that were represented in the analysis (71 of 384 total 2010 census tracts, and 69 of 404 total 1940s census tracts). The 71 present-day census tracts to which the inventoried properties belonged had higher percentage non-Hispanic Black residents (median: 49.7%; interquartile range [IQR]: 16.7–90.2%) compared to census tracts across all of Philadelphia (median: 29.8%; IQR: 9.9–78.8%). Percentages of residents living in poverty, identifying as Hispanic, and reporting less than a high school education were similar in the subset of tracts included in the analysis and across all of Philadelphia's 384 modern-day census tracts. The modern-day census tracts of the properties included in this analysis were more densely populated compared to the entire city (median: 7,493.5 people/km^2; IQR: 5,679.1–10,470.1 vs. median: 6,990.8 people/km^2; IQR: 4287.6–9,903.4). The 69 historical census tracts to which the residential properties belonged had lower percentages of residents who were Black (median: 0.3%; IQR: 0.0–1.4%) as compared to all census tracts across the entire city in 1940 (median: 1.1%; IQR: 0.0–9.6%), but higher percentages who had less than 4 years of high school education (median: 24.6%; IQR: 14.4–34.3% vs. median: 17.5%; IQR: 8.7–31.6%). The historical census tracts included in the analysis were also more densely populated compared to all Philadelphia census tracts in 1940 (median: 10,063.5; IQR: 4881.3–14,283.8 vs. median: 5,354.8; IQR: 630.1–14,141.9).

Table 2 provides descriptive statistics on the 400 properties for which we conducted inventories. Overall, 70.2% of the properties had low (< 25%) or no mature tree canopy cover, and 49.5% had no immature street trees. The majority of properties inventoried were town/row homes (90.5%). Of the 400 properties, 38.2% had a dark roof, 87.8% had a flat roof, and 36.2% had a roof that was both dark and flat. Nearly all (93%) of the properties located in grade A areas were also located in the most racially and

Table 1 Descriptive statistics for the 1940s and 2010 census tracts included in the analysis and across all of Philadelphia, PA

	Tracts included in analysis	All of Philadelphia census tracts
	2010 census tracts	
Total census tracts (*N*)	**71**	**384**
	Median (IQR)	
Total properties per census tract	1 (1–2)	
% Non-Hispanic Black	49.7 (16.7, 90.2)	29.8 (9.9, 78.8)
% Hispanic	4.5 (2.1, 11.0)	6.3 (3.1, 13.4)
% Living in poverty	24.3 (12.9, 39.2)	22.4 (12.7, 36.7)
% Adults with less than a high school education	14.7 (8.0, 22.2)	14.4 (8.2, 20.9)
Population density (population/km^2)	7493.5 (5679.1, 10,470.1)	6990.8 (4287.6, 9903.4)
	1940s census tracts	
Total census tracts	**69**	**404**
	Median (IQR)	
Total properties per census tract	1 (1–2)	
% Black	0.3 (0.0, 1.4)	1.1 (0.0, 9.6)
% Non-White	0.3 (0.1, 1.5)	1.2 (0.1, 10.0)
% Adults with less than a high school education	24.6 (14.4, 34.3)	17.5(8.7, 31.6)
Population density (population/km^2)	10,063.5 (4881.3, 14,283.8)	5354.8 (630.1, 14,141.9)

Table 2 Housing and land cover characteristics of the 400 residential properties, inventoried using aerial and streetside imagery captured in years 2018–2019, Philadelphia, PA

	N (%)
Single family home	30 (7.5)
Town or row home	362 (90.5)
Apartment building	8 (2.0)
Low tree canopy cover	281 (70.2)
No immature street trees	198 (49.5)
Dark, flat roof	145 (36.2)
Flat roof	351 (87.8)
Dark roof	153 (38.2)

socioeconomically deprived areas, based on the contemporary ICE statistic (Supplemental Material 3). By contrast, 75% and 50% of the properties in grade B and C areas, respectively, were located in areas characterized by the lowest levels of modern-day deprivation. A majority (79%) of properties in HOLC grade D areas were in the second-most deprived areas. Percentages of properties with heat vulnerability characteristics increased as levels of present-day racialized socioeconomic segregation increased (Supplemental Material 1). For example, 91.3%, 79.5%, and 50.4% of 127 properties in census tracts with the highest levels of racial/socioeconomic deprivation had low or no tree canopy, no newly planted/immature street trees, and a flat, dark roof, respectively. By contrast, 17.0%, 12%, and 20% of 100 properties in the least deprived (most privileged) tracts had these respective characteristics.

Crude Analytic Results

Figure 1 presents crude relative risk (RR) estimates of association between the HOLC grades (properties in grade B, C, and D neighborhoods, each compared with properties in grade A neighborhoods) and the housing or land cover characteristics. Compared to properties in grade A neighborhoods, higher proportions of properties in grade B, grade C, and grade D areas had the following characteristics, all of which may enhance heat vulnerability: a dark roof, a flat roof, a dark and flat roof, low or no mature tree canopy cover, and no immature street trees. In many cases, proportions of properties with many of the heat vulnerability factors were higher in grade B and C than in grade D neighborhoods, although there was not always a consistent dose–response relationship. For example, compared to properties in grade A neighborhoods, those in grade B neighborhoods had 2.45-fold higher risk of having a flat, dark roof

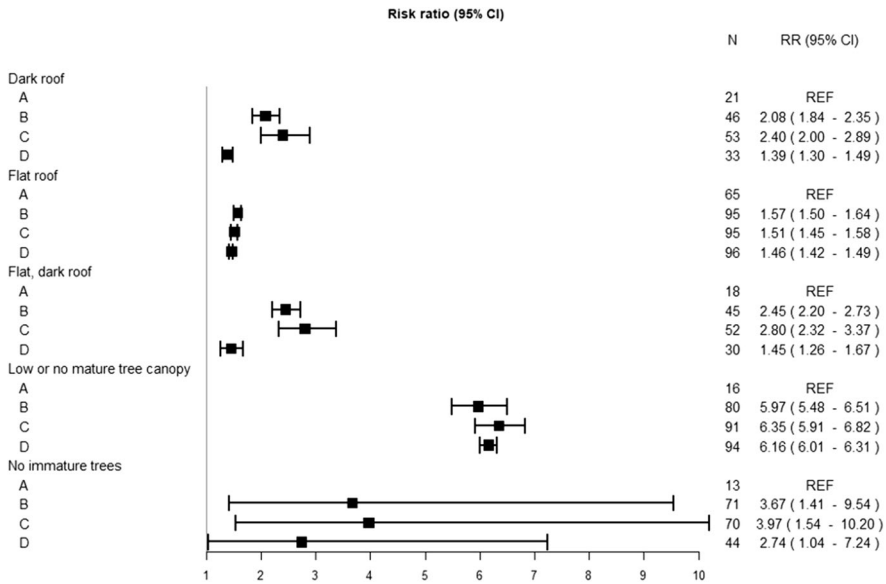

Fig. 1 Crude risk ratio estimates of asssociation comparing the proportion of 100 residential properties in grade B, C, and D vs. grade A areas of Philadelphia, PA, with present-day heat vulnerability enhancing housing or land cover characteristics

(95% CI: 2.20–2.73), and those in grade C neighborhoods had 2.80-fold higher risk (95% CI: 2.32–3.37), while those in grade D neighborhoods had 1.45 times the risk (95% CI: 1.26–1.67). Of all the features, we observed the most substantial contrasts for mature tree canopy cover, with properties in grade B, C, and D neighborhoods having 5.97 (95% CI: 5.48–6.51), 6.35 (95% CI: 5.91–6.82), and 6.16 (95% CI: 6.01–6.31) times the risk of having low/no tree canopy cover compared to those in grade A neighborhoods, respectively.

Analyses Adjusted for Historical Socioeconomic and Racial Deprivation

Adjusting for historical socioeconomic and racial deprivation measures caused estimates of association between HOLC grades and the heat vulnerability characteristics to move towards the null (Fig. 2). After adjustment, associations comparing proportions of properties with dark roofs in grade B, C, and D vs. grade A areas were 1.74 (95% CI: 1.13–2.70), 1.92 (95% CI: 1.11–3.34), and 0.93 (95% CI: 0.38–2.30), respectively (Fig. 2). Associations with lack of immature street trees remained elevated but moved towards the null; the estimate for the grade D to grade A became very imprecise with CIs that crossed the null (moving from RR: 2.74, 95% CI: 1.04–7.24 to RR: 2.31, 95% CI: 0.61–8.70). RR estimates of association with low or no tree canopy were slightly attenuated but remained elevated (e.g., RR for comparisons with grade A: comparing properties to 5.67, 95% CI: 4.06–7.90 for grade B; 5.92, 95% CI: 4.24–8.26 for grade C; and 5.14, 95% CI: 2.76–9.57 for grade D).

Analyses Adjusted for Contemporary Racialized Socioeconomic Deprivation

After adjustment for present-day racialized economic segregation, estimates comparing properties in grade D to grade A areas were relatively unchanged. RR estimates comparing properties in grade B and C areas with properties in grade A areas moved closer to the null compared to the crude estimates, though they remained elevated (Supplemental Material 5).

In sensitivity analyses, results were similar when we specified clustering by 1940s rather than 2010 census tracts (data not shown).

Discussion

In the first study to examine historic redlining practices and contemporary measures of housing heat vulnerability in a major city in the USA, we found that higher proportions of properties in HOLC grade B, C, and D neighborhoods had low or no tree canopy, lacked immature street trees, and had more dark, flat roofs, compared to properties in HOLC grade A neighborhoods. Adjustment for measures of historical

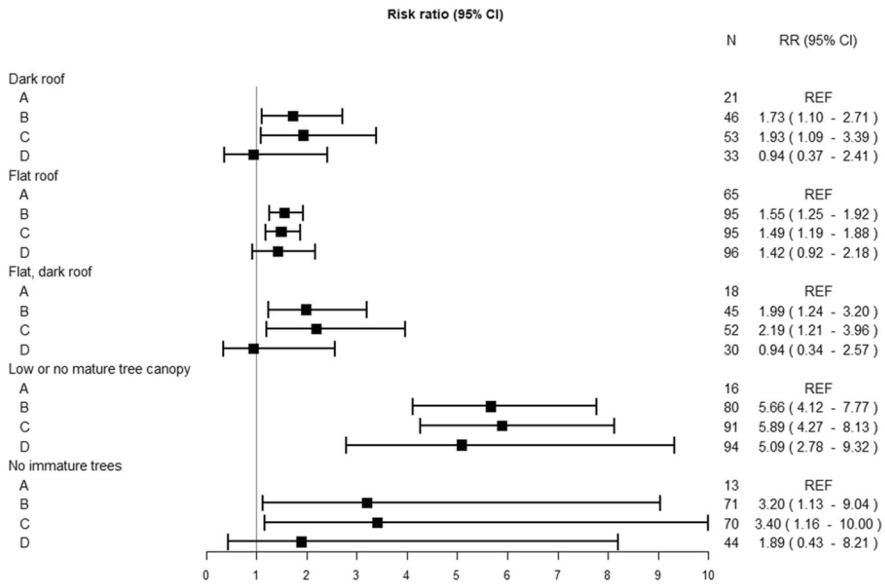

Fig. 2 Risk ratio estimates of asssociation comparing proportion of 100 residential properties in grade B, C, and D vs. grade A areas of Philadelphia, PA, respectively, with present-day heat vulnerability enhancing housing or land cover characteristics, adjusted for neighborhood socioeconomic environment (measured using an index measure combining dimensions of housing environment, educational attainment, and unemployment), and for racialized segregation (measured using the Index of Concentration at the Extremes comparing proportion Black vs. proportion white) in the 1940s

racial deprivation and socioeconomic environment caused nearly all estimates of association to become null and/or to become very imprecise, apart from the estimate of association with mature tree canopy, which remained elevated. After adjustment for present-day racialized socioeconomic deprivation, estimates comparing properties in grade D with grade A areas were unchanged, but contrasts of properties in grades B and C with grade A areas were attenuated, suggesting that present-day racialized economic deprivation may partly explain associations. Overall, these results contribute to a growing body of literature documenting impacts of historic and present-day structural racism on present-day heat vulnerability [47] and land cover and built-environment characteristics that exacerbate heat vulnerability [19, 30, 37].

Philadelphia, PA, is a city with old housing stock, and many of the properties inventoried were constructed before the HOLC maps were established. Nevertheless, decades of neighborhood development following the construction of the properties and the HOLC maps may have led to inequities in property infrastructure and characteristics that align with the historical HOLC grades, or with subsequent patterns of racial residential segregation. The most substantial association we observed was between the HOLC grades and low or no presence of mature tree canopy at or immediately surrounding the property. Mature tree canopy takes years to grow and develop, and resource and asset deprivation that accompanies historical, institutional disinvestment (or neglect) may be best characterized by this community resource compared to housing characteristics, which may experience more change from neighborhood redevelopment and investment over time. Our results related to tree canopy are consistent with previous nation-wide analyses of associations between HOLC grades and tree canopy [48] and greenspace density [37].

HOLC grade ratings were based, in large part, on neighborhood sociodemographic composition, including race [35]. Thus, the sociodemographic of neighborhoods that were in place before the establishment of HOLC maps may partly explain observed associations. Adjustment for historical measures of sociodemographic deprivation caused estimates of association between HOLC grades and the heat vulnerability characteristics to move towards the null. These results are consistent with an analysis of associations between HOLC grades and contemporary

rates of violent crime in Philadelphia, in which associations became null after adjusting for historical sociodemographic compositional measures [36].

Since the creation of the HOLC maps in the late 1930s, there have been shifts in the spatial patterns of deprivation across the city of Philadelphia. These shifts are reflected by the fact that the majority of properties located in HOLC grade A areas are now located in neighborhoods characterized by the highest levels of contemporary racialized socioeconomic deprivation. We hypothesized that historical segregation and historically redlined areas may have impacted present-day racial residential segregation and that present-day racialized economic segregation might be a causal intermediate between the HOLC grades and present-day heat vulnerability characteristics. Even after adjusting for contemporary measures of racialized socioeconomic deprivation, estimates comparing properties in grade D areas with those in grade A areas remained fairly unchanged, while those comparing properties in grade B or grade C areas moved towards the null. These results suggest that contemporary racialized economic deprivation either confounds or explains some of the associations with heat vulnerability characteristics in properties in grade B or grade C areas, but not with properties in grade D areas. The results with respect to grade D areas point to enduring impacts of historical racist systems, even following shifts in the geographic patterns of deprivation.

Strengths of this work include the use of publicly available, high-resolution aerial, and streetside imagery to characterize, at an extremely high spatial resolution, land cover, and structural features of individual properties. Consideration of housing characteristics, such as roof color, that may impact indoor exposures is an important novelty and contribution to research on heat vulnerability. The methods used in this study can be replicated in future empirical research on housing and land cover characteristics that may impact outdoor and indoor temperatures—a potentially important but understudied determinant of heat vulnerability. Nevertheless, we acknowledge several limitations. While streetside and aerial view imagery is an excellent tool for characterizing housing and land cover features at a high resolution, the images represent only single snapshots in time; identification of features is subject to errors that come from user interpretation and photograph obstruction. Another limitation is that we randomly selected properties for assessment from within HOLC grade categories, but did not doubly or triply stratify Philadelphia neighborhoods by categories of present or historical sociodemographics composition, or by population/housing density. As a result, there was little variation in sociodemographic composition variables within (or, surprisingly, even across) grade categories, and results may be biased due to residual confounding. We did not have long-term longitudinal data describing shifts in sociodemographics, urban neighborhood change (including gentrification), and decisions about housing renovation and development. As a result, our data did not meet the strong assumptions needed to estimate causal mediation, including no unmeasured exposure-mediator or mediator-outcome confounding [49], and we did not formally test mediation of the association between HOLC grades and heat vulnerability characteristics by present-day racial residential segregation. This is an important area for future work. We also did not have the statistical power to conduct analyses stratified by categories of contemporary racialized economic deprivation. Adjusting for data from the 1930 decennial census would have been preferable to the 1940 census, since these data would better represent the characteristics of neighborhoods before the HOLC map was established. However, because of data availability, we relied on the 1940s decennial census. We assume that, overall, the sociodemographic composition of neighborhoods in 1930 was similar to that represented by the 1940s decennial census data. Finally, large sections of present-day Philadelphia, some of which are highly racially segregated [30], were not included in the HOLC maps developed in the 1930s. Therefore, results from this analysis illuminate relationships between historical, rather than contemporary racial residential segregation and heat vulnerability. Further work is needed to explore links between contemporary residential racial segregation and heat vulnerability across all sections making up modern-day Philadelphia.

Conclusion

Vulnerability to extreme heat is one of the most critical public health issues of our time. Previous empirical research has showcased vast spatial variability in

the distribution of heat-related mortality rates, with higher rates clustering in only a fraction of neighborhoods from across major US cities, many of which are characterized by high proportion ethnic/racial minorities and people living in poverty [50. In this paper, we explored one potential historical and social explanation for this spatial variability. We analyzed associations between high resolution estimates of residential property characteristics with historical racial segregation and present-day sociodemographic composition. Overall, our results suggest that historically redlined areas are home to present-day housing and land cover features that may enhance heat vulnerability, but the relationship between these historical policies with present-day neighborhood features may be explained by historical and/or present-day neighborhood sociodemographics. Overall, this work highlights climate change as an important issue of environmental justice, [51] and demonstrates that historical HOLC maps are spatial representations of present-day heat vulnerability. Further research with historical data representing changes in neighborhood redevelopment, gentrification, and housing over time is needed to fully understand relationships between structural racism, residential segregation, and heat vulnerability.

Funding American Heart Association,00015611,Leah Schinasi

References

1. Georgescu M, Morefield PE, Bierwagen BG, Weaver CP. Urban adaptation can roll back warming of emerging megapolitan regions. *Proc Natl Acad Sci U S A*. 2014;111(8):2909–14. https://doi.org/10.1073/pnas.1322280111.
2. I. *Climate Change 2021: The Physical Science Basis. Contribution of Working Group I to the Sixth*
3. *Assessment Report of the Intergovernmental Panel on Climate Change*. 2021.
4. Gasparrini A, Guo Y, Sera F, et al. Projections of temperature-related excess mortality under climate change scenarios. *Lancet Planet Health*. 2017;1(9):e360–7. https://doi.org/10.1016/S2542-5196(17)30156-0.
5. Mirchandani HG, McDonald G, Hood IC, Fonseca C. Heat-related deaths in Philadelphia–1993. *Am J Forensic Med Pathol*. 1996;17(2):106–8.
6. Semenza JC, Rubin CH, Falter KH, et al. Heat-related deaths during the July 1995 heat wave in Chicago. *N Engl J Med*. 1996;335(2):84–90. https://doi.org/10.1056/NEJM199607113350203.
7. Laaidi K, Zeghnoun A, Dousset B, et al. The impact of heat islands on mortality in Paris during the August 2003 heat wave. *Environ Health Perspect*. Feb 2012;120(2):254–9.:https://doi.org/10.1289/ehp.1103532
8. Benmarhnia T, Auger N, Stanislas V, Lo E, Kaufman JS. The relationship between apparent temperature and daily number of live births in Montreal. *Maternal and child health journal*. 2015;19(12):2548–51.:https://doi.org/10.1007/s10995-015-1794-y
9. Uejio CK, Wilhelmi OV, Golden JS, Mills DM, Gulino SP, Samenow JP. Intra-urban societal vulnerability to extreme heat: the role of heat exposure and the built environment, socioeconomics, and neighborhood stability. *Health & place*. 2011;17(2):498–507.:https://doi.org/10.1016/j.healthplace.2010.12.005
10. Harlan SL, Brazel AJ, Prashad L, Stefanov WL, Larsen L. Neighborhood microclimates and vulnerability to heat stress. *Social science & medicine*. 2006;63(11):2847–63.:https://doi.org/10.1016/j.socscimed.2006.07.030
11. A. R, Akbari H, Romm JJ, Pomerantz M. PomerantzCool communities: strategies for heat island mitigation and smog reduction. *Energy Build*. 1998;28:51–62.
12. Stone B Jr, Vargo J, Liu P, et al. Avoided heat-related mortality through climate adaptation strategies in three US cities. *PLoS ONE*. 2014;9(6): e100852. https://doi.org/10.1371/journal.pone.0100852.
13. Grimm NB, Faeth SH, Golubiewski NE, et al. Global change and the ecology of cities. *Science*. 2008;319(5864):756–60. https://doi.org/10.1126/science.1150195.
14. Mohajerani A, Bakaric J, Jeffrey-Bailey T. The urban heat island effect, its causes, and mitigation, with reference to the thermal properties of asphalt concrete. *J Environ Manage*. Jul 15 2017;197:522–538.:https://doi.org/10.1016/j.jenvman.2017.03.095
15. Asaeda T, Thanh Ca V, Wake A. Heat storage of pavement and its effect on the lower atmosphere. *Atmos Environ*. 1996;30(3):413–27.
16. Oke TR. The energetic basis of the urban heat-island. *Q J Roy Meteor Soc*. 1982;108(455):1–24. https://doi.org/10.1002/qj.49710845502.
17. Fouillet A, Rey G, Laurent F, et al. Excess mortality related to the August 2003 heat wave in France. *Int Arch Occup Environ Health*. 2006;80(1):16–24. https://doi.org/10.1007/s00420-006-0089-4.
18. Centers for Disease C, Prevention. Heat-related deaths--Philadelphia and United States, 1993–1994. *MMWR Morbidity and mortality weekly report*. Jul 1 1994;43(25):453–5.
19. Klepeis NE, Nelson WC, Ott WR, et al. The National Human Activity Pattern Survey (NHAPS): a resource for assessing exposure to environmental pollutants. *J Expo Anal Environ Epidemiol*. 2001;11(3):231–52. https://doi.org/10.1038/sj.jea.7500165.
20. Casey JA, James P, Cushing L, Jesdale BM, Morello-Frosch R. Race, ethnicity, income concentration and 10-year change in urban greenness in the United States. *Int J Environ Res Public Health*. 2017;14(12):https://doi.org/10.3390/ijerph14121546
21. Jesdale BM, Morello-Frosch R, Cushing L. The racial/ethnic distribution of heat risk-related land cover in

relation to residential segregation. *Environ Health Perspect*. 2013;121(7):811–7.:https://doi.org/10.1289/ehp.1205919
22. Faber JW. We built this: consequences of new deal era intervention in American's racial geography. *Am Sociol Rev*. 2020;85(5):739–75.
23. Barber S, Diez Roux AV, Cardoso L, et al. At the intersection of place, race, and health in Brazil: residential segregation and cardio-metabolic risk factors in the Brazilian Longitudinal Study of Adult Health (ELSA-Brasil). *Social science & medicine*. 2018;199:67–76.:https://doi.org/10.1016/j.socscimed.2017.05.047
24. Anguelovski I, Connolly J, Pearsall H, et al. Opinion: why green "climate gentrification" threatens poor and vulnerable populations. *Proc Natl Acad Sci U S A*. 2019;52:26138–43. https://doi.org/10.1073/pnas.1920490117.
25. Mayne SL, Loizzo L, Bancks MP, et al. Racial residential segregation, racial discrimination, and diabetes: the Coronary Artery Risk Development in Young Adults study. *Health Place*. 2020;62: 102286. https://doi.org/10.1016/j.healthplace.2020.102286.
26. Williams DR, Collins C. Racial residential segregation: a fundamental cause of racial disparities in health. *Public Health Rep*. 2001;116(5):404–16. https://doi.org/10.1093/phr/116.5.404.
27. Nardone A, Casey JA, Morello-Frosch R, Mujahid M, Balmes JR, Thakur N. Associations between historical residential redlining and current age-adjusted rates of emergency department visits due to asthma across eight cities in California: an ecological study. *Lancet Planet Health*. 2020;4(1):e24–31. https://doi.org/10.1016/S2542-5196(19)30241-4.
28. Nardone AL, Casey JA, Rudolph KE, Karasek D, Mujahid M, Morello-Frosch R. Associations between historical redlining and birth outcomes from 2006 through 2015 in California. *PLoS ONE*. 2020;15(8): e0237241. https://doi.org/10.1371/journal.pone.0237241.
29. Krieger N, Van Wye G, Huynh M, et al. Structural racism, historical redlining, and risk of preterm birth in New York City, 2013–2017. *Am J Public Health*. 2020;110(7):1046–53. https://doi.org/10.2105/AJPH.2020.305656.
30. Krieger N, Wright E, Chen JT, Waterman PD, Huntley ER, Arcaya M. Cancer Stage at diagnosis, historical redlining, and current neighborhood characteristics: breast, cervical, lung, and colorectal cancers, Massachusetts, 2001–2015. *Am J Epidemiol*. 2020;189(10):1065–75. https://doi.org/10.1093/aje/kwaa045.
31. Barber S, Headen I, Branch B, Tabb L, Yadeta K. *Covid-19 in context: racism, segregation, and racial inequities in Philadelphia*. 2020. 2020. https://drexel.edu/uhc/resources/briefs/Covid-19%20in%20Context/. Accessed 30 Jun 2021.
32. From the Centers for Disease Control and Prevention. Heat-related deaths–Philadelphia and United States, 1993–1994. *JAMA*. 1994;272(3):197.
33. USCB. Census Bureau Glossary. https://www.census.gov/programs-surveys/geography/about/glossary.html#par_textimage_13. Accessed 30 Jun 2021.
34. Nelson RK, Winling L, Marciano R, Connolly N, al. e. Mapping inequality. https://dsl.richmond.edu/panorama/redlining/#loc=5/39.1/-94.58&text=downloads. Accessed 30 Jun 2021.
35. City of Philadelphia Office of Property Assessment. *OpenDataPhilly: Property Assessments*. 2016;
36. Hillier A. Redlining and the home owners' loan corporation. *J Urban Hist*. 2003;29(4):394–420. https://doi.org/10.1177/0096144203029004002.
37. Jacoby SF, Dong B, Beard JH, Wiebe DJ, Morrison CN. The enduring impact of historical and structural racism on urban violence in Philadelphia. *Soc Sci Med*. 2018;199:87–95. https://doi.org/10.1016/j.socscimed.2017.05.038.
38. Nardone A, Rudolph KE, Morello-Frosch R, Casey JA. Redlines and Greenspace: the Relationship between Historical Redlining and 2010 Greenspace across the United States. *Environ Health Perspect*. 2021;129(1):17006. https://doi.org/10.1289/EHP7495.
39. Manson S, Schroeder j, Van Riper D, Kugler T, Ruggles S. IPUMS National Historical Geographic Information System: Version 15.0. [1940_tPH_Major]. *Minneapolis, MN: IPUMS*. 2020; http://doi.org/https://doi.org/10.18128/D050.V15.0
40. Krieger N, Waterman PD, Spasojevic J, Li W, Maduro G, Van Wye G. Public health monitoring of privilege and deprivation with the index of concentration at the extremes. *Am J Public Health*. 2016;106(2):256–63. https://doi.org/10.2105/AJPH.2015.302955.
41. Diez Roux AV, Merkin SS, Arnett D, et al. Neighborhood of residence and incidence of coronary heart disease. *N Engl J Med*. 12 2001;345(2):99–106. https://doi.org/10.1056/NEJM200107123450205
42. USCB. Geographic Areas Reference Manual. Chapter 10. Census tracts and block numbering areas. In: USDoC, ed. *Geographic Areas Reference Manual* 1994.
43. Bureau USC. American Community Survey (ACS). January 27, 2016. Accessed 2016, 2016. https://www.census.gov/programs-surveys/acs/
44. Blasnik M. *Impact Evaluation of the Energy Coordinating Agency of Philadelphia's Cool Homes Pilot Project*. 2004. https://www.coolrooftoolkit.org/wp-content/uploads/2012/04/Blasnik-2004-Eval-coolhomes_Philly-EAC.pdf. Accessed 30 Jun 2021.
45. Jenerette GD, Harlan SL, Buyantuev A, et al. Micro-scale urban surface temperatures are related to land-cover features and residential heat related health impacts in Phoenix. *AZ USA Landscape Ecology*. 2016;31(4):745–60. https://doi.org/10.1007/s10980-015-0284-3.
46. Zou G. A modified poisson regression approach to prospective studies with binary data. *Am J Epidemiol*. 2004;159(7):702–6. https://doi.org/10.1093/aje/kwh090.
47. Halekoh U, Hojgaard S, Yan J. The R Package geepack for generalized estimationg equations. *J Stat Softw*. 2006;15(2):1–11.
48. Hoffman JS, Shandas V, Pendleton N. The effects of historical housing policies on resident exposure to intra-urban heat: a study of 108 US urban areas. *Climate*. 2020;8(12)(1) https://doi.org/10.3390/cli8010012
49. Locke DH, Hall BJ, Grove M, et al. Residential housing segregation and urban tree canopy in 37 US Cities. *Urban Sustainability*. 2021. https://doi.org/10.1038/s42949-021-00022-0.

50. VanderWeele TJ. Mediation analysis: a practitioner's guide. *Annu Rev Public Health*. 2016;37:17–32. https://doi.org/10.1146/annurev-publhealth-032315-021402.
51. Hondula DM, Davis RE, Saha MV, Wegner CR, Veazey LM. Geographic dimensions of heat-related mortality in seven U.S. cities. *Environ Res*. 2015;138:439–52. https://doi.org/10.1016/j.envres.2015.02.033
52. Mulholland M. A moment of intersecting crises: climate justice in the era of coronavirus. *Development (Rome)*. 2020:1–5. https://doi.org/10.1057/s41301-020-00259-9